PROCEEDINGS OF SCIENCE

Exploring Sterile Neutrino and Non-Unitary Neutrino Mixing at nuSTORM

Kaustav Chakraborty,[a,*] **Srubabati Goswami**[a] **and Kenneth R. Long**[b,c]

[a] *Theoretical Physics Division, Physical Research Laboratory, Ahmedabad - 380009, India*
[b] *Department of Physics, Imperial College London, Exhibition Road, SW7 2AZ, UK*
[c] *STFC Rutherford Appleton Laboratory,Harwell Campus, Didcot, OX11 0QX, UK*

E-mail: kaustav@prl.res.in, sruba@prl.res.in, k.long@imperial.ac.uk

The Neutrinos from Stored muons (nuSTORM) facility has been proposed to measure neutrino-nucleon cross-sections with percent level precision. It has been shown that nuSTORM with a detector for short baseline oscillation search has excellent capability to search for the existence of light sterile neutrinos that have been postulated to explain the LSND and MiniBooNE results. This analysis used the Charged Current events in a magnetized Iron calorimeter detector. We study if the large number of Neutral Current events at the detector can be used to constrain the sterile neutrino parameter space further. In addition we also study the constraints on non-unitarity of neutrino mixing matrix using both charged and neutral current events at nuSTORM.

**** The 22nd International Workshop on Neutrinos from Accelerators (NuFact2021) ****
**** 6–11 Sep 2021 ****
**** Cagliari, Italy ****

[*] Speaker

PoS(NuFact2021)178

1. Introduction

Neutrino oscillation is an important field of research which have established the paradigm of the three-flavour neutrino oscillations. The neutrino mass hierarchy, the octant of θ_{23} and δ_{CP} are expected to be determined in the near future with the currently running and proposed high statistics experiments. Additionally, it is interesting to study the capabilities of these experiments to explore the new physics scenarios like light sterile neutrinos, non-unitarity of the neutrino mixing matrix, non-standard interactions of the neutrinos etc.

The LSND results [1] led to the postulation of existence of light sterile neutrinos. The experiment reported signals of $\nu_\mu - \nu_e$ which could be accounted to neutrino oscillations with mass-squared difference of the order of eV^2. The result was seconded by MiniBooNE [2] and then subsequently by the gallium and reactor anomalies [3]. The 3+1 neutrino mixing scenario provides an acceptable fit to the data [4]. But, there exists a between disappearance and appearance data which is driven mainly by ν_μ disappearance data and the LSND appearance data [5] with contribution also coming from MiniBooNE appearance although it is subleading. The contribution for the tension in disappearance data comes from from CDHS [6], MINOS/MINOS+ [7], SK [8], IceCube DeepCore [9], MiniBooNE, NOνA [10]. Hence, it is essential to probe such new physics scenarios in present and future high statistics experiments. In this regards nuSTORM [11, 12] facility provides a unique perspective due to its beam originating from muon decay process: $\mu^+ \rightarrow e^+\nu_e\overline{\nu}_\mu$ with 50% ν_e and 50% $\overline{\nu}_\mu$ which can give e^-. The scenarios regarding sterile neutrinos and non-unitary neutrino mixing has been explored in [13].

2. Experimental and Simulation Details

The experiment has been simulated by following the configuration and detector simulations from [11, 12]. We performed simulation using the General Long Baseline Experiment Simulator (GLoBES) package[14, 15]. The flux in fig.1 is obtained from the decay $\mu^+ \rightarrow e^+ + \nu_e + \bar{\nu}_\mu$ with a neutrino beam containing 50 GeV protons with 2×10^{21} protons on target over the duration of 10 years. Pions of 5 GeV are injected into the muon storage ring. Muons with energy of the order 3.8 GeV subsequently decay to give ν_e and $\bar{\nu}_\mu$. The ν_e flux peaks at 2.5 GeV whereas the $\bar{\nu}_\mu$ flux peaks at 3 GeV. nuSTORM is simulated as described in [11, 12] .

The detector chosen is a 1.3 kt magnetized iron-scintillator calorimeter which has excellent charge selection and detection characteristics for muons. The channels relevant to the experiment are $\nu_e \rightarrow \nu_\mu$ appearance channel and $\bar{\nu}_\mu \rightarrow \bar{\nu}_\mu$ disappearance channel. The events in i^{th} energy bin are calculated as

$$n_\alpha^i = \frac{N}{L^2} \int_{E_i - \frac{\Delta E_i}{2}}^{E_i + \frac{\Delta E_i}{2}} dE' \int_0^\infty \varepsilon(E)\phi_\beta(E)P_{\alpha\beta}(E)\sigma_\alpha(E)R^c(E,E')\varepsilon^c(E')dE \tag{1}$$

where, E denotes the true neutrino energy and E' denotes the measured neutrino energy. $R^c(E,E')$ denotes the smearing matrix, which relates the true and the measured energy.

The statistical χ^2_{stat} is calculated assuming Poisson distribution,

$$\chi^2_{stat} = \sum_i 2\left(N_i^{test} - N_i^{true} - N_i^{true}\log\frac{N_i^{test}}{N_i^{true}}\right). \tag{2}$$

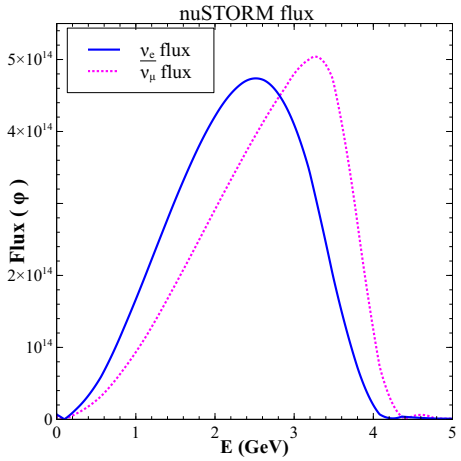

Figure 1: The unoscillated ν_e and $\bar{\nu}_\mu$ flux extracted from the storage ring. The flux is evaluated for (3.8±0.38) GeV/c muon decay at a distance of 2 km[11].

Here, 'i' stands for the number of bins and N_i^{test}, N_i^{true} stands for total number of test and true events respectively.

3. Results

Sterile Neutrino : Since we are in the short baseline regime with distance of ∼2 km and $E \sim$ 3 GeV, the "One Mass Scale Dominance" (OMSD) approximation is valid. The system is and an effective two-generation where the oscillation probabilities can be obtained as,

$$P_{e\mu} = 4\cos^2\theta_{14}\sin^2\theta_{14}\sin^2\theta_{24}\sin^2\left(\frac{\Delta m^2_{41}L}{4E}\right) \quad (3)$$

$$P_{\mu\mu} = 1 - 4\sin^2\theta_{24}\cos^2\theta_{14}(1-\sin^2\theta_{24}\cos^2\theta_{14})\sin^2\left(\frac{\Delta m^2_{41}L}{4E}\right) \quad (4)$$

$$P_{es} + P_{\mu s} = 4\cos^4\theta_{14}\cos^2\theta_{24}\cos^2\theta_{34}(\sin^2\theta_{14}+\sin^2\theta_{24})\sin^2\left(\frac{\Delta m^2_{41}L}{4E}\right) \quad (5)$$

The fig.2 presents the θ_{14}, θ_{24} and θ_{34} bounds predicted from nuSTORM. We can conclude from this study that nuSTORM will be capable to test θ_{14}, θ_{24} upto 6° and 7.5° respectively. It is clear from the figure that the inclusion of NC events can put stringent bounds on both θ_{14} and θ_{24}. The second and third plots in the figure describes the effect of nuSTORM to constrain θ_{14} and θ_{24} with respect to θ_{34}. Taking all the channels into account both θ_{14} and θ_{24} can be approximately constrained upto 4° at nuSTORM. In both the plots it is clear that the charged current interaction are independent of θ_{34} which is also understood from the expressions of $P_{e\mu}$ and $P_{\bar{\mu}\bar{\mu}}$. The only dependence on θ_{34} can come from the neutral current channel. But $P_{e\mu} + P_{\bar{\mu}\bar{\mu}} \propto \cos^2\theta_{34}$ as a result of which there is weak dependence of θ_{34} on the neutral current events hence θ_{34} cannot be constrained by neutral current events in nuSTORM.

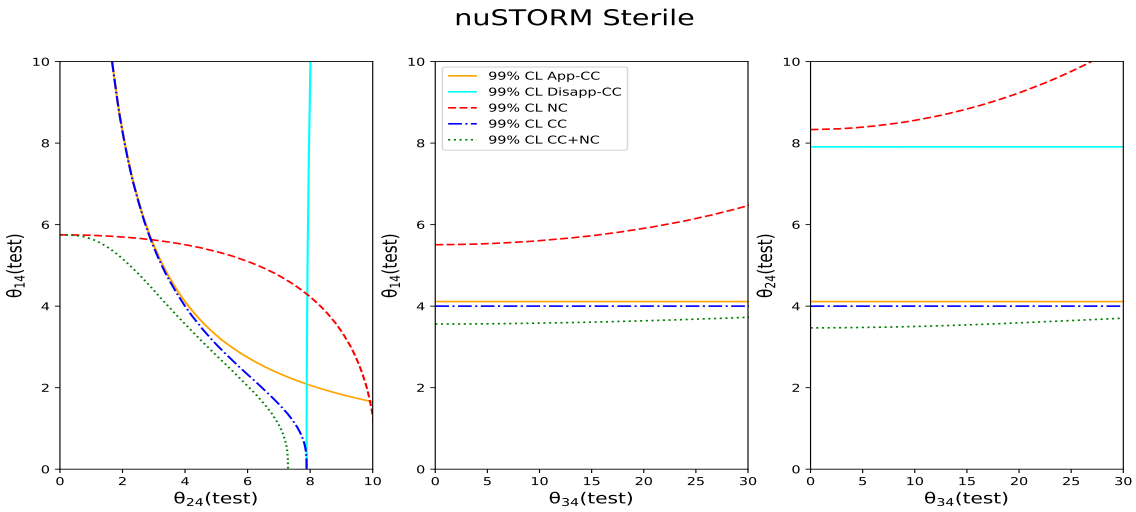

Figure 2: The testable regions for sterile neutrinos as predicted by nuSTORM for $\Delta m^2_{41} = 1\text{ev}^2$ and baseline of 2 km in terms of θ_{14}, θ_{24} and θ_{34} bounds. The first, second and third plots present the θ_{14}(test) vs θ_{24}(test), θ_{14}(test) vs θ_{34}(test) and θ_{24}(test) vs θ_{34}(test) contours respectively. Each plot consists of 5 contours of 99% confidence level significance exclusion regions for various channels as labeled in the plots.

Non-Unitary Mixing : In the framework of non-unitary neutrino mixing the mixing matrix N can be parametrized as:

$$N = N^{NP}U = \begin{bmatrix} \alpha_{11} & 0 & 0 \\ \alpha_{21} & \alpha_{22} & 0 \\ \alpha_{31} & \alpha_{32} & \alpha_{33} \end{bmatrix} U; \tag{6}$$

where U is the PMNS matrix, N^{NP} is the left triangle matrix which portrays non unitarity. The diagonal elements in the matrix N^{NP} are real but the off diagonal elements are allowed to be complex.

$$P_{e\mu} = \alpha_{11}^2|\alpha_{21}|^2, \qquad P_{\mu\mu} = (|\alpha_{21}|^2 + \alpha_{22}^2)^2 \tag{7}$$

$$P_{es} + P_{\mu s} = 2 - (\alpha_{11}^2(\alpha_{11}^2 + 2|\alpha_{21}|^2 + |\alpha_{31}|^2) + \alpha_{22}^2(\alpha_{22}^2 + 2|\alpha_{21}|^2 + |\alpha_{32}|^2)) \tag{8}$$

The first plot in the Fig.3 presents the sensitivity of nuSTORM to probe the parameter α_{11} keeping $|\alpha_{21}|$ and α_{22} fixed at 0.1 and 1.0 respectively. In the Fig.3 the χ^2 vs $|\alpha_{21}|$ sensitivity has been studied considering both the other non unitarity parameters to α_{11} and α_{22} taken to be unity. Under such conditions $P_{\mu e}$ just reduces to $|\alpha_{21}|^2$ due to which we get the quadratic dependence of the χ^2 vs $|\alpha_{21}|$. From the figure we can conclude that the sensitivity is not conclusive for lower values of $|\alpha_{21}|$ but as we proceed towards higher $|\alpha_{21}|$ values the sensitivity improves and reaches 3σ for $|\alpha_{21}| \sim 0.3$ for the combined case of CC+NC. Similarly, if analyze the right panel of the Fig.3, representing χ^2 vs α_{22} at nuSTORM. This analysis has been performed considering

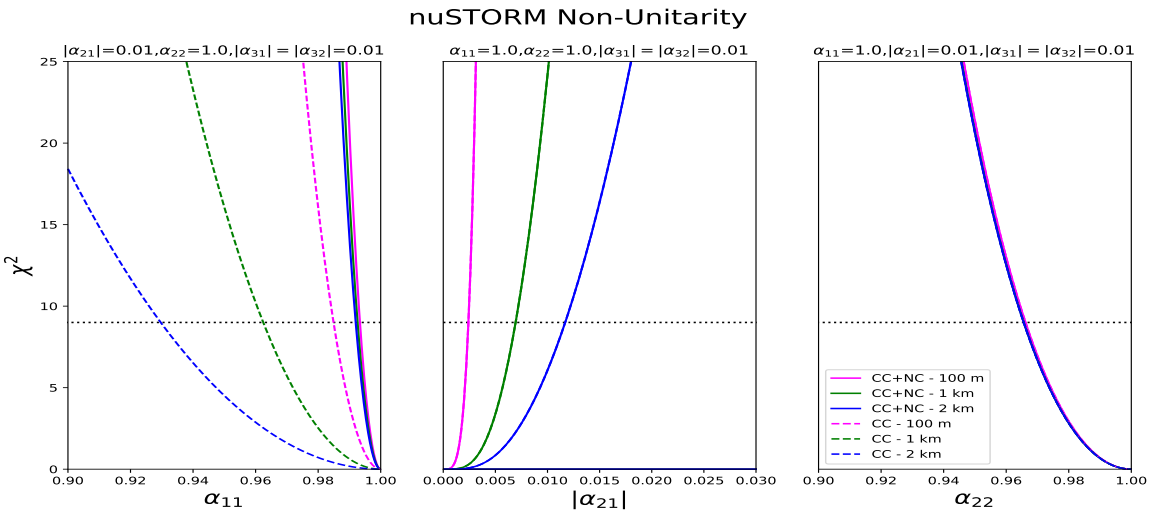

Figure 3: The figure shows the sensitivity to nuSTORM for the non unitarity parameters α_{11}, $|\alpha_{21}|$ and α_{22}. The y-axis in the plots represent χ^2, while the x-axis denotes α_{11}, $|\alpha_{21}|$ and α_{22} for plots respectively. In each plot the dashed lines are for the contribution of only charge current interactions while the solid lines are for the combination of charge current and neutral current. The magenta, green and blue curves represent the sensitivities at the baseline of 100 m, 1 km and 2 km respectively.

$\alpha_{11} = 1.0$ and $|\alpha_{21}| = 0.2$. In this case the sensitivity solely comes from the $P_{\mu\mu}$ channel, and for small values for $|\alpha_{21}|$, $P_{\mu\mu} \sim \alpha_{22}^4$. The α_{22} sensitivity is low for values of α_{22} close to unity and it increases as α_{22} deviates from the unitarity condition, with χ^2 reaching 3σ for $\alpha_{22} \sim 0.96$.

4. Conclusions

nuSTORM will prove to be crucial in investigating the LSND/MiniBOONE anomalies. The experiment will have the capability to study $P_{\mu e}$, $P_{\bar{\mu}\bar{\mu}}$ channels with the proposed MIND detector. The Charged Current interactions to detect the appearance and disappearance channels can constrain the mixing angles θ_{14} and θ_{24}. Introduction of neutral current enhances the capability of nuSTORM to probe the parameters. Especially we observe that for non-zero values of θ_{24}, the constraint on θ_{14} also improves with inclusion of NC events. nuSTORM can probe the non-unitarity parameters α_{11}, $|\alpha_{21}|$ and α_{22}. 3σ sensitivities for α_{11}, $|\alpha_{21}|$ and α_{22} are obtained at 0.995, 0.06 and 0.97 respectively for 2 km baselines combining both CC and NC events.

References

[1] **LSND** Collaboration, A. Aguilar-Arevalo *et al.*, "Evidence for neutrino oscillations from the observation of anti-neutrino(electron) appearance in a anti-neutrino(muon) beam," *Phys. Rev.* **D64** (2001) 112007, arXiv:hep-ex/0104049 [hep-ex].

[2] **MiniBooNE** Collaboration, A. A. Aguilar-Arevalo *et al.*, "Significant Excess of ElectronLike Events in the MiniBooNE Short-Baseline Neutrino Experiment," *Phys. Rev. Lett.* **121** no. 22, (2018) 221801, arXiv:1805.12028 [hep-ex].

[3] G. Mention, M. Fechner, T. Lasserre, T. A. Mueller, D. Lhuillier, M. Cribier, and A. Letourneau, "The Reactor Antineutrino Anomaly," *Phys. Rev.* **D83** (2011) 073006, arXiv:1101.2755 [hep-ex].

[4] M. Dentler, Hernández-Cabezudo, J. Kopp, P. A. Machado, M. Maltoni, I. Martinez-Soler, and T. Schwetz, "Updated Global Analysis of Neutrino Oscillations in the Presence of eV-Scale Sterile Neutrinos," *JHEP* **08** (2018) 010, arXiv:1803.10661 [hep-ph].

[5] A. Diaz, C. A. Argüelles, G. H. Collin, J. M. Conrad, and M. H. Shaevitz, "Where Are We With Light Sterile Neutrinos?," *Phys. Rept.* **884** (2020) 1–59, arXiv:1906.00045 [hep-ex].

[6] F. Dydak *et al.*, "A Search for Muon-neutrino Oscillations in the Delta m**2 Range 0.3-eV**2 to 90-eV**2," *Phys. Lett. B* **134** (1984) 281.

[7] **MINOS** Collaboration, P. Adamson *et al.*, "Active to sterile neutrino mixing limits from neutral-current interactions in MINOS," *Phys. Rev. Lett.* **107** (2011) 011802, arXiv:1104.3922 [hep-ex].

[8] **Super-Kamiokande** Collaboration, K. Abe *et al.*, "Limits on sterile neutrino mixing using atmospheric neutrinos in Super-Kamiokande," *Phys. Rev.* **D91** (2015) 052019, arXiv:1410.2008 [hep-ex].

[9] **IceCube** Collaboration, M. G. Aartsen *et al.*, "Search for sterile neutrino mixing using three years of IceCube DeepCore data," *Phys. Rev.* **D95** no. 11, (2017) 112002, arXiv:1702.05160 [hep-ex].

[10] **NOvA** Collaboration, P. Adamson *et al.*, "Search for active-sterile neutrino mixing using neutral-current interactions in NOvA," *Phys. Rev.* **D96** no. 7, (2017) 072006, arXiv:1706.04592 [hep-ex].

[11] C. D. Tunnell, "Sterile Neutrino Sensitivity with Wrong-Sign Muon Appearance at nuSTORM," arXiv:1205.6338 [hep-ph].

[12] **nuSTORM** Collaboration, D. Adey *et al.*, "Light sterile neutrino sensitivity at the nuSTORM facility," *Phys. Rev.* **D89** no. 7, (2014) 071301, arXiv:1402.5250 [hep-ex].

[13] K. Chakraborty, S. Goswami, and K. Long, "New physics at nuSTORM," *Phys. Rev. D* **103** no. 7, (2021) 075009, arXiv:2007.03321 [hep-ph].

[14] P. Huber, M. Lindner, and W. Winter, "Simulation of long-baseline neutrino oscillation experiments with GLoBES," *Comput. Phys. Commun.* **167** (2005) 195, arXiv:hep-ph/0407333. %%CITATION = HEP-PH/0407333;%%.

[15] P. Huber, J. Kopp, M. Lindner, M. Rolinec, and W. Winter, "New features in the simulation of neutrino oscillation experiments with GLoBES 3.0" *Comput. Phys. Commun.* **177** (2007) 432–438, arXiv:hep-ph/0701187. %%CITATION = HEP-PH/0701187;%%.